Earth Reinforcement, Ochiai, Yasufuku & Omine (eds) © 1996 Balkema, Rotterdam. ISBN 90 5410 833 9

Shear-lag analysis of a geosynthetic reinforced soil wall

Luis Claudio Rosa da Silva & Mauricio Abramento
Instituto de Pesquisas Tecnológicas do Estado de São Paulo, Brazil

ABSTRACT: This paper presents a method for verifying the performance of reinforced soil walls under working load conditions, using an analytical model based on shear-lag formulation. The theoretical results predicted from the model are compared with experimental results obtained from a prototype reinforced soil wall, which employs sandy soil reinforced with geogrid layers. The paper presents details on the procedure for applying the analytical model, the reference parameters for the analysis, the results obtained with the model and an analysis of the influence of these parameters. The results show that the analytical model can predict with accuracy the load distribution along the reinforcement layers.

1 INTRODUCTION

Current design methods for reinforced soil masses are based primarily on limit equilibrium analyses (e.g. Jewell, 1990). Stability of the structure is maintained either through sliding resistance along the soil-reinforcement interface or through tensile stresses generated in the reinforcement, resisted by an anchor length embedded in the stable soil mass (i.e., pullout mode). However, limit equilibrium calculations are not adequate for estimating the magnitude and distribution of reinforcement stresses at working load conditions. For example, Bathurst et al. (1988) have built and carefully instrumented a 3,0m high prototype geosynthetic reinforced soil wall at the Royal Military College (RMC), Canada, in order to study in details the performance of such structures, employing different face configurations and construction procedures. The results showed that predictions (by other researchers) of stresses and strains along the reinforcements as well as displacements of wall face using limit equilibrium calculations were radically different from those measured in the experiments. In one of the RMC experiments, four layers of Tensar SR-2 geogrid 3,0m long were used as reinforcing element for a sandy soil. The geogrids, with an average spacing of 0.75m, were connected to the wall face. The RMC wall was fully instrumented, so that strains along the reinforcement as well as displacements at the face could be monitored during construction and surcharge loading (of 12, 30, 40 and 50kPa). Different face elements were used to verify the influence of construction method on the wall behavior (incremental or propped methods).

This paper will focus on the analysis and interpretation of load distribution along the inclusions for the RMC propped wall tests results, using the shear-lag model (Abramento and Whittle, 1993). The model, summarized below, is capable of predicting the complete load distribution for an element of reinforced soil. This paper constitutes the first adaptation of the shear-lag model for estimating stresses along inclusions in a reinforced soil wall.

2 ADAPTATION OF SHEAR-LAG MODEL

Figure 1 shows the geometry for a composite plane strain element of reinforced soil considered in the analysis. It comprises a planar inclusion of thickness, f, and length, L, embedded in a soil matrix of overall height, m (inclusion spacing). Abramento and Whittle (1993) presented an elastic analytical method, based on shear-lag analysis, for estimating the tensile stresses in a single planar reinforcement due to shearing of the surrounding soil matrix. The analysis expresses reinforcement stresses as closed form functions of the inclusion geometry (f, m, L), elastic properties of the constituent materials (soil and reinforcement) and level of external stresses. In the original formulation, the inclusion is parallel to the minor, external, principal stress on the soil matrix, $\sigma_3=\sigma_h$ (i.e., $\theta=0$ in Figure 1).

Abramento (1993) has modified the basic formulation in order to consider other orientations of principal stresses ($\theta\neq0$ in Fig. 1), while Abramento and Whittle (1995) considered pullout conditions of the inclusion ($\sigma_p\neq0$ in Figure 1). The analytical expressions are summarized as follows.

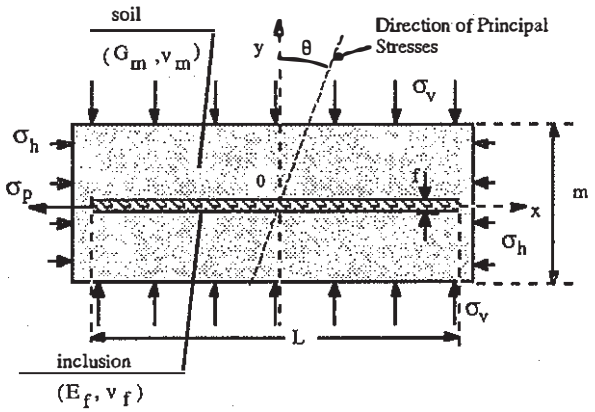

Fig. 1 Geometry for an element of reinforced soil

The axial inclusion stresses due to compression only of the soil mass ($\sigma_{xx}^{f,c}$, with $\sigma_p=0$ and $\sigma_h;\sigma_v\neq 0$) is given by:

$$\sigma_{xx}^{f,c} = \frac{K_2}{K_1}\left[1 - \frac{\cosh\left(\sqrt{K_1}\,x\right)}{\cosh\left(\sqrt{K_1}\,\frac{L}{2}\right)}\right] \quad (1)$$

The axial inclusion stresses due to pullout mode only of the inclusion ($\sigma_{xx}^{f,p}$, with $\sigma_p\neq 0$ and $\sigma_h=\sigma_v=0$) is given by:

$$\sigma_{xx}^{f,p} = \sigma_p \frac{\sinh\left[\sqrt{K_3}\left(\frac{L}{2} - x\right)\right]}{\sinh\left(\sqrt{K_3}\,L\right)} \quad (2)$$

In these expressions, K_1, K_2 and K_3 are written in terms of material properties, geometry and state of stress in the soil matrix:

$$K_1 = \left[\frac{6\cos\theta}{m\,f\,(1+0.25\,\nu_m)}\right]\left[\frac{f}{m}\left(\cos\theta - \frac{\nu_m}{\cos\theta}\right) + 2\frac{G_m}{E_f}\right] \quad (3)$$

$$K_2 = \left[\frac{6\cos\theta}{mf(1+0.25\nu_m)}\right]\left[\left(\nu_m - \sin^2\theta\right)\sigma_v + \left(\nu_m - \cos^2\theta\right)\sigma_h\right] \quad (4)$$

$$K_3 = \left[\frac{6}{m\,f\,(1+0.25\,\nu_m)}\right]\left[\frac{f}{m}(1-\nu_m) + 2\frac{G_m}{E_f}\right] \quad (5)$$

Expression 3 to 5 are presented in a simplified form, and are valid for: a) $\nu_f \rightarrow 0$ (since the influence of ν_f on the stress distribution is very small); b) neglecting shear stresses at the boundary of the reinforced element in Figure 1; and c) small values of θ (geometric limitation). Abramento (1993) generalizes these expressions for any values of θ and ν_f, and also considering shear stresses acting at the boundary of the soil mass.

The following hypothesis were considered in order to apply the shear-lag model for analyzing the RMC prototype reinforced soil wall: 1) The elements of reinforced soil can be stacked in order to produce a "reinforced wall", and each layer can be independently analyzed using the shear-lag formulation; 2) There are no shear stresses acting along the boundary of different layers of these elements; and 3) The axial stresses due to pullout conditions of the inclusion ($\sigma_{xx}^{f,p}$) and compression conditions of the soil matrix ($\sigma_{xx}^{f,c}$) can be independently determined and added together for determining the total stress distribution along the inclusion.

3 PARAMETERS USED IN THE ANALYSIS

The shear-lag analysis derives the axial inclusion stress (σ_{xx}^{f}) as functions of the exterior soil stresses (σ_v, σ_h, θ, σ_p), material properties (E_f, G_m, ν_f, ν_m) and geometry (f, m, L). In order to apply the shear-lag analysis for the RMC prototype reinforced wall, the parameters were estimated as follows and are summarized in Table 1:

1) Soil elastic parameters G_m and ν_m: Bathurst et al. (1988) measured very small values of strains in the reinforcement even for the highest value of surcharge (e.g., 0,9%, for the top layer with q=50kPa, after 1,000 hours). These results suggest that the overall strains prevailing within the reinforced mass were very small. Therefore, soil elastic parameters were obtained from the early part of stress-strain curves for the sand used in the tests.

2) Inclusion elastic parameters E_f and ν_f: The reinforcement elastic modulus E_f was obtained by dividing its rigidity J by the smallest (rib) thickness, f=1,34mm (which controls the geogrid deformation; Bathurst et al., 1988). The value of J was calculated for the isocronous loading of 1,000h (close to the minimum running time for all tests), supposing linear variation of strain in the early portion (0 to 1%) of the load-strain curve; ν_f was taken as 0.2, but it has negligible influence on the stress distribution.

3) Geometry: The smallest geogrid thickness f=1.34mm was considered, since it controls its strain; the inclusion spacing m was taken, respectively, as 0.88m, 0.75m, 0.75m and 0.62m, for the fourth, third, second and first layers of geogrid, from the top to the bottom of the wall. The total inclusion length L=3,0m was not considered in the analysis. Instead, an "effective length" (L_e) was fitted to the results, as discussed ahead in section 4.

4) State of stress in the soil matrix: This is the most difficult condition to estimate in order to apply the shear-lag analysis. The state of stress is characterized by the vertical and horizontal stresses in the soil mass (σ_v, σ_h) as well as their rotation with vertical direction (θ). The shear-lag analysis assumes an uniform state of stress in the soil matrix; in contrast, the state of stresses in the wall is highly non-uniform. Conditions close to rest, K_0, are expected far from wall face,

whereas active conditions are expected close to the wall face. Therefore, the average state of stress was determined as follows:

The vertical stress in the soil matrix σ_v was considered as $\sigma_v=\gamma z_i+q$, where γ is the unit weight of sand (17.5kN/m^3), q is the surcharge at the wall top, and z_i is the depth of the i-th geogrid layer (i.e., z_i=0.50, 1.25, 2.00 and 2.75m for the 4th, 3rd, 2nd and 1st geogrid layers (from the top to the bottom of the wall). The horizontal stress in the soil mass σ_h was calculated as $\sigma_h=K_a\sigma_v$, where K_a is the coefficient of active stress given by the Coulomb formulation. For computation of K_a, the peak friction angle of sand ϕ_p was considered, and the wall-soil friction was taken as $\delta=2\phi_p/3$.

The pullout stress σ_p was determined assuming the lateral pressure distribution at wall face proposed by Terzaghi (1936):

$$\sigma_p=\frac{m}{f}K_a\left[1+\alpha\left(1-\frac{z_i}{H}\right)\right]\left\{\frac{H\gamma}{\alpha}+\left(q-\frac{H\gamma}{\alpha}\right)\exp\left[-\frac{\alpha z_i}{H}\right]\right\} \quad (6)$$

Where H=3.0m is the wall height and the parameter α was taken as α=1.30 (Murray et al., 1990).

Rotation of stresses with vertical direction θ was varied to better fit the results, as follows.

Table 1. Parameters used in the shear-lag analysis.

Properties of Sand and Reinforcement		
Property	Sand	Reinforcement
Elastic Modulus	G_m=3.3MPa	E_f=400MPa
Poisson	ν_m=0.5	ν_f=0.2
Thickness	m=0.62 to 0.88	f=1.34mm
Length	-	L_e=0.75 to 3.0m
Friction Angle	ϕ=53°	-

4 RESULTS

Figures 2 and 3 present comparisons between experimental results measured by Bathurst et al. (1988) in the RMC prototype reinforced wall and the shear-lag solutions. The comparisons concentrate in the load distribution along the inclusions, for two values of surcharge (q=12kPa and q=50kPa in Figs. 2 and 3, respectively). Due to the difficulty in estimating the complete stress field in the soil matrix, two parameters were varied to better fit the experimental results: the rotation of stresses with the vertical direction θ and the inclusion length L, resulting in an "effective inclusion length", L=L_e. The results show that:

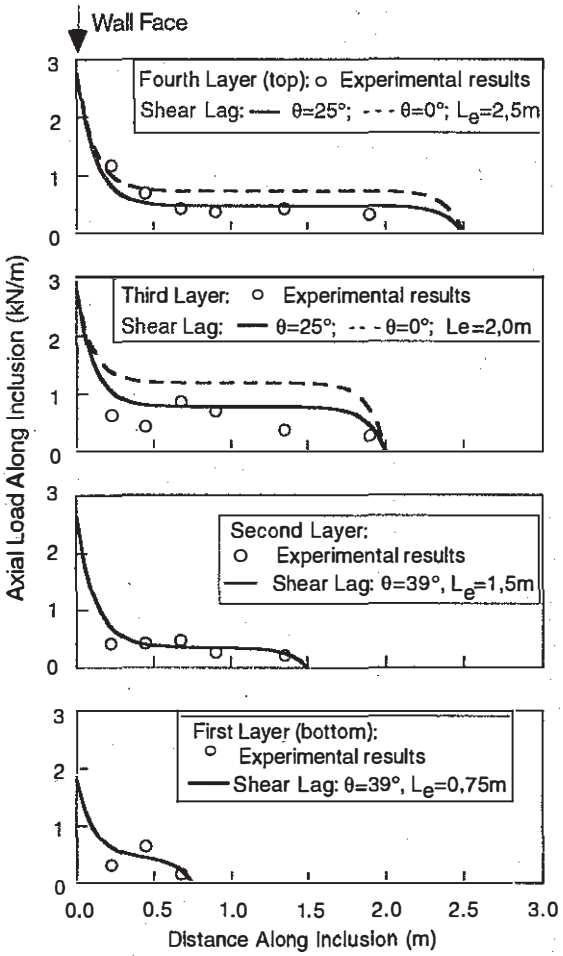

Fig.2 Experimental results vs. shear-lag analysis for 12kPa surcharge

1) There is generally very good agreement between measured and predicted results, for both load level and distribution.

2) The pullout stress σ_p controls the load distribution in the reinforcements close to the wall face. The shear-lag analysis predicts higher tensile loads in the inclusions close to the wall face, under working load conditions. Near failure, however, it is expected that the peak tensile loads should approach the failure surface in the soil mass (e.g. Tatsuoka, 1992).

3) Best fit of results was obtained for principal stress rotations of θ=0 to 25° for the two top layers and θ=35° to 39° for the two bottom layers. These values are in agreement with those observed by other researchers (e.g. Rowe and Ho, 1992). Large rotation of principal stresses towards the bottom of wall causes a significant reduction in the axial inclusion stresses.

4) Rotation of stresses is also reflected in the decrease of "effective length" L_e for the bottom layers, indicating that the reinforcement is not being fully loaded. In particular, the stresses for the lowest (1st)

layer are due almost exclusively to pullout conditions σ_p. This indicates that the bottom reinforcement layers are not oriented in the direction of maximum benefit, i.e., in the direction of principal tensile strains.

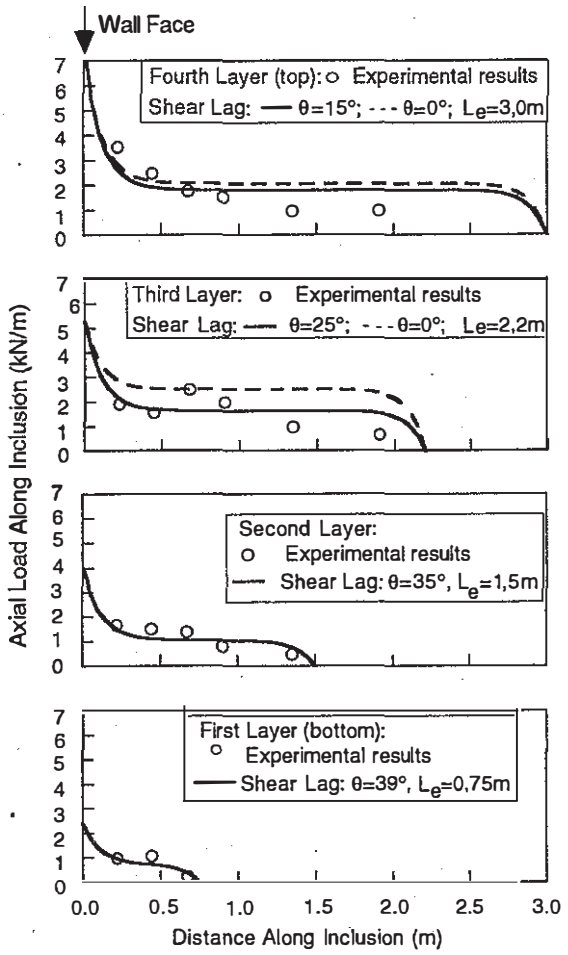

Fig.3 Experimental results vs. shear-lag analysis for 50kPa surcharge

5 CONCLUSIONS

This paper presents the first adaptation of the shear-lag analysis for interpreting and quantifying the stress distribution along the reinforcements in a prototype reinforced soil wall. The parameters involved in the analysis can be estimated from conventional laboratory tests. To overcome the problem of highly non-uniform state of stress within the reinforced soil mass, a simple stress distribution was considered, supposing active conditions in the soil. The analysis showed that there is significant rotation of stresses towards the toe of the wall, and at this location the bottom reinforcement layers are not oriented in the direction of maximum benefit, i.e., in the direction of principal tensile strains. The shear-lag model constitutes a very simple and direct method for assessing the influence of the many parameters involved in the analysis. The shear-lag solution may be modified in order to consider a more complex state of stress in the soil mass. For example, Beech (1987) suggests subdividing the reinforced soil mass in different regions, each one with a homogeneous state of stress, and determining stresses and strains in the soil and reinforcement through superposition. Silva (1996) presents an extensive parametric study using the shear-lag model to fully interpret stresses along the inclusions as well as face displacements of two RMC (propped and incremental faces) reinforced walls.

REFERENCES

Abramento, M. & Whittle, A.J. 1995. Analysis of Pullout Tests for Planar Reinforcements in Soil. *ASCE Journal of Geotechnical Engineering*, 121(6), June, 476-485.

Abramento, M. & Whittle, A.J. 1993. Shear-Lag Analysis of a Planar Soil Reinforcement in Plane Strain Compression. *ASCE Journal of Engineering Mechanics*, 119(2), 270-291.

Abramento, M. 1993. *Analysis and Measurement of Stresses in Planar Soil Reinforcements*. Ph.D. Thesis, Dep. of Civil and Environmental Engineering, Massachusetts Institute of Technology, Cambridge, 288p.

Bathurst, R.J.; Wawrychuck, W.F. & Jarret, P.M. 1988. Laboratory Investigation of Two Large-Scale Geogrid Reinforced Soil Walls. *The Application of Polymeric Reinforcement in Soil Retaining Structures*. Proc. NATO Advanced Research Workshop, Kingston, Kluwer Publishers, 71-125.

Beech, J.F. 1987. Importance of Stress-Strain Relationships in Reinforced Soil Systems Designs. *Geosynthetics '87*, New Orleans, 133-144.

Jewell, R. A. 1990. Strength and Deformation in Reinforced Soil Design. *Proc. 4th Intl. Conf. on Geotextiles, Geomembranes and Related Products*, The Hague.

Murray, R.T.; Andrawes, K.Z. & McGown, A. 1990. Design, Construction and Performance of Reinforced Soil Walls. *Proc. Intern. Conf. on Geotextiles, Geomembranes and Related Products*, The Hage, 1003-1007.

Rowe, R.K. & Ho, S.K. 1992. A Review of the Behavior of Reinforced Soil Walls. *Int. Symp. on Earth Reinf. Practice*, Kyushu '92, 47-76.

Silva, L.C.R. 1996. *Analysis of a Reinforced Soil Wall under Working Load Conditions*. M.Sc. Thesis, Escola Politécnica da Universidade de São Paulo (in Portuguese), Brazil, 180p.

Tatsuoka, F. 1992. Roles of Facing Rigidity in Soil Reinforcement. *Int.Symp. on Earth Reinforcement Practice*, Kyushu '92, 77-115.

Terzaghi, K. 1936. Distribution of the Lateral Pressure of Sand on the Timbering of Cuts. *Proc. I Intern. Conf. Soil Mech. and Found. Eng.*, Harvard, 1, 211-215.